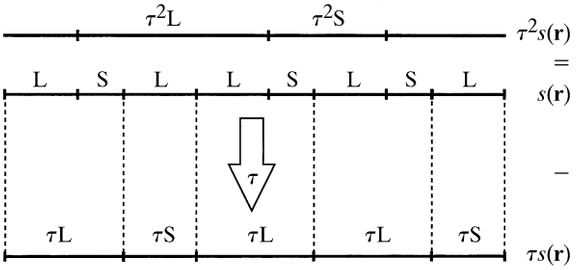

Fig. 4.6.3.10. Part ... LSLLSLSL ... of a Fibonacci sequence $s(\mathbf{r})$ before and after scaling by the factor τ. L is mapped onto τL, S onto τS = L. The vertices of the new sequence are a subset of those of the original sequence (the correspondence is indicated by dashed lines). The residual vertices $\tau^2 s(\mathbf{r})$, which give when decorating $\tau s(\mathbf{r})$ the Fibonacci sequence $s(\mathbf{r})$, form a Fibonacci sequence scaled by a factor τ^2.

$$F(\mathbf{H}) = F(\tau\mathbf{H}) + \exp(2\pi i\tau\mathbf{H})F(\tau^2\mathbf{H}).$$

Hence, phases of structure factors that are related by scaling symmetry can be determined from each other.

Further scaling relationships in reciprocal space exist: scaling a diffraction vector

$$\mathbf{H} = h_1\mathbf{d}_1^* + h_2\mathbf{d}_2^* = h_1 a^* \begin{pmatrix} 1 \\ -\tau \end{pmatrix}_V + h_2 a^* \begin{pmatrix} \tau \\ 1 \end{pmatrix}_V$$

with the matrix

$$S = \begin{pmatrix} 0 & 1 \\ 1 & 1 \end{pmatrix}_D,$$

$$\begin{aligned} \begin{pmatrix} 0 & 1 \\ 1 & 1 \end{pmatrix}_D \begin{pmatrix} h_1 \\ h_2 \end{pmatrix}_D &= \begin{pmatrix} F_n & F_{n+1} \\ F_{n+1} & F_{n+2} \end{pmatrix}_D \begin{pmatrix} h_1 \\ h_2 \end{pmatrix}_D \\ &= \begin{pmatrix} F_n h_1 + F_{n+1} h_2 \\ F_{n+1} h_1 + F_{n+2} h_2 \end{pmatrix}_D, \end{aligned}$$

increases the magnitudes of structure factors assigned to this particular diffraction vector $\mathbf{H}$,

$$\left|F(S^n\mathbf{H})\right| > \left|F(S^{n-1}\mathbf{H})\right| > \ldots > \left|F(S\mathbf{H})\right| > \left|F(\mathbf{H})\right|.$$

This is due to the shrinking of the perpendicular-space component of the diffraction vector by powers of $(-\tau)^{-n}$ while expanding the parallel-space component by τ^n according to the eigenvalues τ and $-\tau^{-1}$ of S acting in the two eigenspaces $\mathbf{V}^{\parallel}$ and $\mathbf{V}^{\perp}$:

$$\begin{aligned} \pi^{\parallel}(S\mathbf{H}) &= (h_2 + \tau(h_1 + h_2))a^* = (\tau h_1 + h_2(\tau + 1))a^* \\ &= \tau(h_1 + \tau h_2)a^*, \\ \pi^{\perp}(S\mathbf{H}) &= (-\tau h_2 + h_1 + h_2)a^* = (h_1 - h_2(\tau - 1))a^* \\ &= -(1/\tau)(-\tau h_1 + h_2)a^*, \\ \left|F(\tau^n\mathbf{H}^{\parallel})\right| &> \left|F(\tau^{n-1}\mathbf{H}^{\parallel})\right| > \ldots > \left|F(\tau\mathbf{H}^{\parallel})\right| > \left|F(\mathbf{H}^{\parallel})\right|. \end{aligned}$$

Thus, for scaling n times we obtain

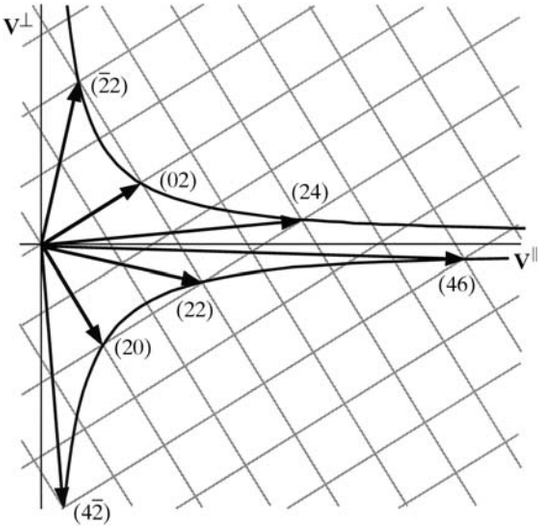

Fig. 4.6.3.11. Scaling operations of the Fibonacci sequence. The scaling operation S acts six times on the diffraction vector $\mathbf{H} = (4\bar{2})$ yielding the sequence $(4\bar{2}) \rightarrow (\bar{2}2) \rightarrow (20) \rightarrow (02) \rightarrow (22) \rightarrow (24) \rightarrow (46)$.

$$\begin{aligned} \pi^{\perp}(S^n\mathbf{H}) &= \left(-\tau\left(F_n h_1 + F_{n+1} h_2\right) + \left(F_{n+1} h_1 + F_{n+2} h_2\right)\right)a^* \\ &= \left(h_1\left(-\tau F_n + F_{n+1}\right) + h_2\left(-\tau F_{n+1} + F_{n+2}\right)\right)a^* \end{aligned}$$

with

$$\lim_{n\to\infty}\left(-\tau F_n + F_{n+1}\right) = 0 \text{ and } \lim_{n\to\infty}\left(-\tau F_{n+1} + F_{n+2}\right) = 0,$$

yielding eventually

$$\lim_{n\to\infty}\left(\pi^{\perp}(S^n\mathbf{H})\right) = 0 \text{ and } \lim_{n\to\infty}\left(F(S^n\mathbf{H})\right) = F(\mathbf{0}).$$

The scaling of the diffraction vectors $\mathbf{H}$ by S^n corresponds to a hyperbolic rotation (Janner, 1992) with angle $n\varphi$, where $\sinh\varphi = 1/2$ (Fig. 4.6.3.11):

$$\begin{pmatrix} 0 & 1 \\ 1 & 1 \end{pmatrix}^{2n} = \begin{pmatrix} \cosh 2n\varphi & \sinh 2n\varphi \\ \sinh 2n\varphi & \cosh 2n\varphi \end{pmatrix},$$

$$\begin{pmatrix} 0 & 1 \\ 1 & 1 \end{pmatrix}^{2n+1} = \begin{pmatrix} \sinh[(2n+1)\varphi] & \cosh[(2n+1)\varphi] \\ \cosh[(2n+1)\varphi] & \sinh[(2n+1)\varphi] \end{pmatrix}.$$

4.6.3.3.2. Decagonal phases

A structure quasiperiodic in two dimensions, periodic in the third dimension and with decagonal diffraction symmetry is called a decagonal phase. Its holohedral Laue symmetry group is $K = 10/mmm$. All reciprocal-space vectors $\mathbf{H} \in M^*$ can be represented on a basis (V basis) $\mathbf{a}_i^* = a_i^*(\cos 2\pi i/5, \sin 2\pi i/5, 0)$, $i = 1, \ldots, 4$ and $\mathbf{a}_5^* = a_5^*(0, 0, 1)$ (Fig. 4.6.3.12) as $\mathbf{H} = \sum_{i=1}^{5} h_i\mathbf{a}_i^*$. The vector components refer to a Cartesian coordinate system in physical (parallel) space. Thus, from the number of independent reciprocal-basis vectors necessary to index the Bragg reflections with integer numbers, the dimension of the embedding space has to be at least five. This can also be shown in a different way (Hermann, 1949).

The set M^* of all vectors $\mathbf{H}$ remains invariant under the action of the symmetry operators of the point group $10/mmm$. The symmetry-adapted matrix representations for the point-group

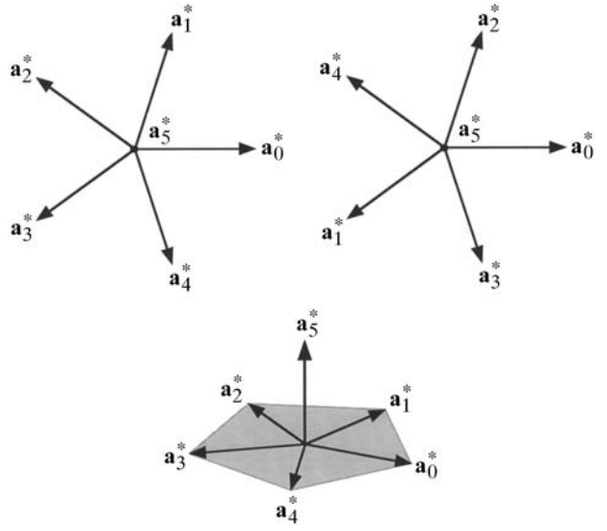

Fig. 4.6.3.12. Reciprocal basis of the decagonal phase in the 5D description projected upon $\mathbf{V}^{\parallel}$ (above left) and $\mathbf{V}^{\perp}$ (above right). Below, a perspective physical-space view is shown.

generators, the tenfold rotation $\alpha = 10$, the reflection plane $\beta = m_2$ (normal of the reflection plane along the vectors $\mathbf{a}_i^*$–$\mathbf{a}_{i+3}^*$ with $i = 1, \ldots, 4$ modulo 5) and the inversion operation $\Gamma(\gamma) = \bar{1}$ may be written in the form

$$\Gamma(\alpha) = \begin{pmatrix} 0 & 1 & \bar{1} & 0 & 0 \\ 0 & 1 & 0 & \bar{1} & 0 \\ 0 & 1 & 0 & 0 & 0 \\ \bar{1} & 1 & 0 & 0 & 0 \\ 0 & 0 & 0 & 0 & 1 \end{pmatrix}_D \quad \Gamma(\beta) = \begin{pmatrix} 0 & 0 & 0 & 1 & 0 \\ 0 & 0 & 1 & 0 & 0 \\ 0 & 1 & 0 & 0 & 0 \\ 1 & 0 & 0 & 0 & 0 \\ 0 & 0 & 0 & 0 & 1 \end{pmatrix}_D$$

$$\Gamma(\gamma) = \begin{pmatrix} \bar{1} & 0 & 0 & 0 & 0 \\ 0 & \bar{1} & 0 & 0 & 0 \\ 0 & 0 & \bar{1} & 0 & 0 \\ 0 & 0 & 0 & \bar{1} & 0 \\ 0 & 0 & 0 & 0 & \bar{1} \end{pmatrix}_D .$$

By block-diagonalization, these reducible symmetry matrices can be decomposed into non-equivalent irreducible representations. These can be assigned to the two orthogonal subspaces forming the 5D embedding space $\mathbf{V} = \mathbf{V}^{\parallel} \oplus \mathbf{V}^{\perp}$, the 3D parallel (physical) subspace $\mathbf{V}^{\parallel}$ and the perpendicular 2D subspace $\mathbf{V}^{\perp}$. Thus, using $W\Gamma W^{-1} = \Gamma_V = \Gamma_V^{\parallel} \oplus \Gamma_V^{\perp}$, we obtain

$$\Gamma_V(\alpha) = \left(\begin{array}{ccc|cc} \cos(\pi/5) & -\sin(\pi/5) & 0 & 0 & 0 \\ \sin(\pi/5) & \cos(\pi/5) & 0 & 0 & 0 \\ 0 & 0 & 1 & 0 & 0 \\ \hline 0 & 0 & 0 & \cos(3\pi/5) & -\sin(3\pi/5) \\ 0 & 0 & 0 & \sin(3\pi/5) & \cos(3\pi/5) \end{array}\right)_V$$

$$= \left(\begin{array}{c|c} \Gamma^{\parallel}(\alpha) & 0 \\ \hline 0 & \Gamma^{\perp}(\alpha) \end{array}\right)_V ,$$

$$\Gamma_V(\beta) = \left(\begin{array}{ccc|cc} 1 & 0 & 0 & 0 & 0 \\ 0 & \bar{1} & 0 & 0 & 0 \\ 0 & 0 & 1 & 0 & 0 \\ \hline 0 & 0 & 0 & 1 & 0 \\ 0 & 0 & 0 & 0 & \bar{1} \end{array}\right)_V , \quad \Gamma_V(\gamma) \left(\begin{array}{ccc|cc} \bar{1} & 0 & 0 & 0 & 0 \\ 0 & \bar{1} & 0 & 0 & 0 \\ 0 & 0 & \bar{1} & 0 & 0 \\ \hline 0 & 0 & 0 & \bar{1} & 0 \\ 0 & 0 & 0 & 0 & \bar{1} \end{array}\right)_V ,$$

where

$$W = \left(\begin{array}{ccccc} a_1^* \cos(2\pi/5) & a_2^* \cos(4\pi/5) & a_3^* \cos(6\pi/5) & a_4^* \cos(8\pi/5) & 0 \\ a_1^* \sin(2\pi/5) & a_2^* \sin(4\pi/5) & a_3^* \sin(6\pi/5) & a_4^* \sin(8\pi/5) & 0 \\ 0 & 0 & 0 & 0 & a_5^* \\ \hline a_1^* \cos(6\pi/5) & a_2^* \cos(2\pi/5) & a_3^* \cos(8\pi/5) & a_4^* \cos(4\pi/5) & 0 \\ a_1^* \sin(6\pi/5) & a_2^* \sin(2\pi/5) & a_3^* \sin(8\pi/5) & a_4^* \sin(4\pi/5) & 0 \end{array}\right).$$

The column vectors of the matrix W give the parallel- (above the partition line) and perpendicular-space components (below the partition line) of a reciprocal basis in V space. Thus, W can be rewritten using the physical-space reciprocal basis defined above as

$$W = \left(\mathbf{d}_1^*, \quad \mathbf{d}_2^*, \quad \mathbf{d}_3^*, \quad \mathbf{d}_4^*, \quad \mathbf{d}_5^*\right),$$

yielding the reciprocal basis $\mathbf{d}_i^*, i = 1, \ldots, 5$, in the 5D embedding space (D space):

$$\mathbf{d}_i^* = a_i^* \begin{pmatrix} \cos(2\pi i/5) \\ \sin(2\pi i/5) \\ 0 \\ \cos(6\pi i/5) \\ \sin(6\pi i/5) \end{pmatrix}_V , \; i = 1, \ldots, 4 \text{ and } \mathbf{d}_5^* = a_5^* \begin{pmatrix} 0 \\ 0 \\ 1 \\ 0 \\ 0 \end{pmatrix}_V .$$

The 5×5 symmetry matrices can each be decomposed into a 3×3 matrix and a 2×2 matrix. The first one, $\Gamma^{\parallel}$, acts on the parallel-space component, the second one, $\Gamma^{\perp}$, on the perpendicular-space component. In the case of $\Gamma(\alpha)$, the coupling factor between a rotation in parallel and perpendicular space is 3. Thus, a $\pi/5$ rotation in physical space is related to a $3\pi/5$ rotation in perpendicular space (Fig. 4.6.3.12).

With the condition $\mathbf{d}_i \cdot \mathbf{d}_j^* = \delta_{ij}$, a basis in direct 5D space is obtained:

$$\mathbf{d}_i = \frac{2}{5a_i^*} \begin{pmatrix} \cos(2\pi i/5) - 1 \\ \sin(2\pi i/5) \\ 0 \\ \cos(6\pi i/5) - 1 \\ \sin(6\pi i/5) \end{pmatrix}, \; i = 1, \ldots, 4, \text{ and } \mathbf{d}_5 = \frac{1}{a_5^*} \begin{pmatrix} 0 \\ 0 \\ 1 \\ 0 \\ 0 \end{pmatrix}.$$

The metric tensors G, G^* are of the type

$$\begin{pmatrix} A & C & C & C & 0 \\ C & A & C & C & 0 \\ C & C & A & C & 0 \\ C & C & C & A & 0 \\ 0 & 0 & 0 & 0 & B \end{pmatrix}$$

with $A = 2a_1^{*2}$, $B = a_5^{*2}$, $C = -(1/2)a_1^{*2}$ for the reciprocal space and $A = 4/5a_1^{*2}$, $B = 1/a_5^{*2}$, $C = 2/5a_1^{*2}$ for the direct space. Thus, for the lattice parameters in reciprocal space we obtain $d_i^* = a_i^*(2)^{1/2}$, $i = 1, \ldots, 4$; $d_5^* = a_5^*$; $\alpha_{ij}^* = 104.5^\circ$, $i, j = 1, \ldots, 4$; $\alpha_{i5}^* = 90^\circ$, $i = 1, \ldots, 4$, and for those in direct space $d_i = 2/[a_i^*(5)^{1/2}]$, $i = 1, \ldots, 4$; $d_5 = 1/a_5^*$; $\alpha_{ij} = 60^\circ$, $i, j = 1, \ldots, 4$; $\alpha_{i5} = 90^\circ$, $i = 1, \ldots, 4$. The volume of the 5D unit cell can be calculated from the metric tensor G:

$$V = [\det(G)]^{1/2} = \frac{4}{5(5)^{1/2}(a_1^*)^4 a_5^*} = \frac{(5)^{1/2}}{4}(d_1)^4 d_5.$$

Since decagonal phases are only quasiperiodic in two dimensions, it is sufficient to demonstrate their characteristics on a 2D

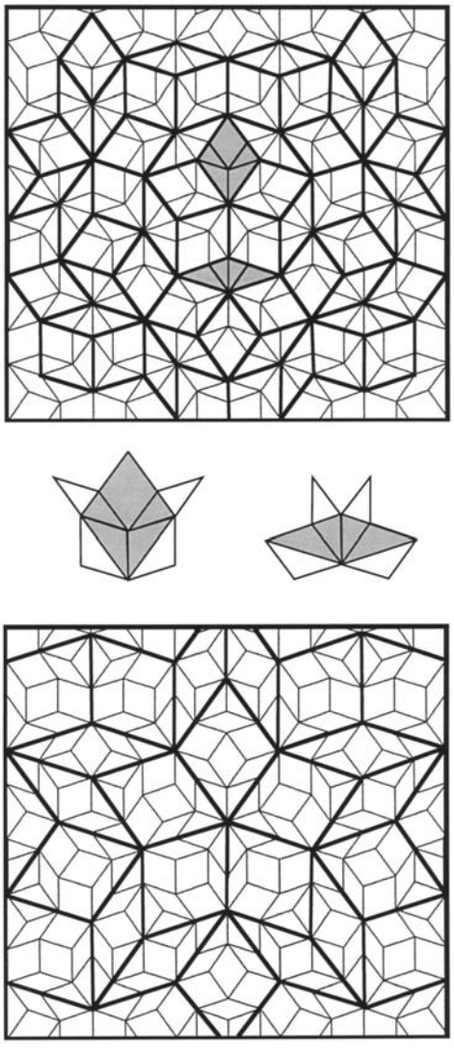

Fig. 4.6.3.13. A section of a Penrose tiling (thin lines) superposed by its τ-deflated tiling (above, thick lines) and by its τ^2-deflated tiling (below, thick lines). In the middle, the inflation rule of the Penrose tiling is illustrated.

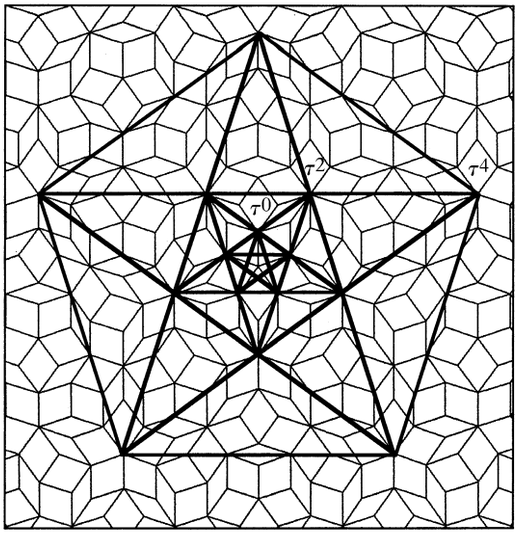

Fig. 4.6.3.14. Scaling symmetry of a pentagram superposed on the Penrose tiling. A vector pointing to a corner of a pentagon (star) is mapped by the rotoscaling operation (rotation around $\pi/5$ and dilatation by a factor τ^2) onto the next largest pentagon (star).

example, the canonical *Penrose tiling* (Penrose, 1974). It can be constructed from two unit tiles: a skinny (acute angle $\alpha_s = \pi/5$) and a fat (acute angle $\alpha_f = 2\pi/5$) rhomb with equal edge lengths a_r and areas $A_S = a_r^2 \sin(\pi/5)$, $A_F = a_r^2 \sin(2\pi/5)$ (Fig. 4.6.3.13). The areas and frequencies of these two unit tiles in the Penrose tiling are both in a ratio 1 to τ. By replacing each skinny and fat rhomb according to the inflation rule, a τ-inflated tiling is obtained. Inflation (deflation) means that the number of tiles is inflated (deflated), their edge lengths are decreased (increased) by a factor τ. By infinite repetition of this inflation operation, an infinite Penrose tiling is generated. Consequently, this substitution operation leaves the tiling invariant.

From Fig. 4.6.3.13 it can be seen that the sets of vertices of the deflated tilings are subsets of the set of vertices of the original tiling. The τ-deflated tiling is dual to the original tiling; a further deflation by a factor τ gives the original tiling again. However, the edge lengths of the tiles are increased by a factor τ^2, and the tiling is rotated around 36°. Only the fourth deflation of the original tiling yields the original tiling in its original orientation but with all lengths multiplied by a factor τ^4.

Contrary to the reciprocal-space scaling behaviour of $M^* = \{\mathbf{H}^{\parallel} = \sum_{i=1}^{4} h_i \mathbf{a}_i^* | h_i \in \mathbb{Z}\}$, the set of vertices $M = \{\mathbf{r} = \sum_{i=1}^{4} n_i \mathbf{a}_i | n_i \in \mathbb{Z}\}$ of the Penrose tiling is not invariant by scaling the length scale simply by a factor τ using the scaling matrix S:

$$S = \begin{pmatrix} 0 & 1 & 0 & \bar{1} \\ 0 & 1 & 1 & \bar{1} \\ \bar{1} & 1 & 1 & 0 \\ \bar{1} & 0 & 1 & 0 \end{pmatrix}_D \text{ acting on vectors } \mathbf{r} = \begin{pmatrix} n_1 \\ n_2 \\ n_3 \\ n_4 \end{pmatrix}_D .$$

The square of S, however, maps all vertices of the Penrose tiling upon other ones:

$$S^2 = \begin{pmatrix} 1 & 1 & 0 & \bar{1} \\ 0 & 2 & 1 & \bar{1} \\ \bar{1} & 1 & 2 & 0 \\ \bar{1} & 0 & 1 & 1 \end{pmatrix}_D , \quad \Gamma(\alpha)S^2 = \begin{pmatrix} 1 & 1 & \bar{1} & \bar{1} \\ 1 & 2 & 0 & \bar{2} \\ 0 & 2 & 1 & \bar{1} \\ \bar{1} & 1 & 1 & 0 \end{pmatrix}_D .$$

S^2 corresponds to a hyperbolic rotation with $\chi = \cosh^{-1}(3/2)$ in superspace (Janner, 1992). However, only operations of the type S^{4n}, $n = 0, 1, 2 \ldots$, scale the Penrose tiling in a way which is equivalent to the ($4n$th) substitutional operations discussed above. The rotoscaling operation $\Gamma(\alpha)S^2$, also a symmetry operation of the Penrose tiling, leaves a pentagram invariant as demonstrated in Fig. 4.6.3.14 (Janner, 1992). Block-diagonalization of the scaling matrix S decomposes it into two non-equivalent irreducible representations which give the scaling properties in the two orthogonal subspaces of the 4D embedding space, $\mathbf{V} = \mathbf{V}^{\parallel} \oplus \mathbf{V}^{\perp}$, the 2D parallel (physical) subspace $\mathbf{V}^{\parallel}$ and the perpendicular 2D subspace $\mathbf{V}^{\perp}$. Thus, using $WSW^{-1} = S_V = S_V^{\parallel} \oplus S_V^{\perp}$, we obtain

$$S_V = \left(\begin{array}{cc|cc} \tau & 0 & 0 & 0 \\ 0 & \tau & 0 & 0 \\ \hline 0 & 0 & -1/\tau & 0 \\ 0 & 0 & 0 & -1/\tau \end{array}\right)_V = \left(\begin{array}{cc|cc} S_V^{\parallel} & & 0 & \\ & & & \\ \hline 0 & & S_V^{\perp} & \end{array}\right)_V ,$$

where

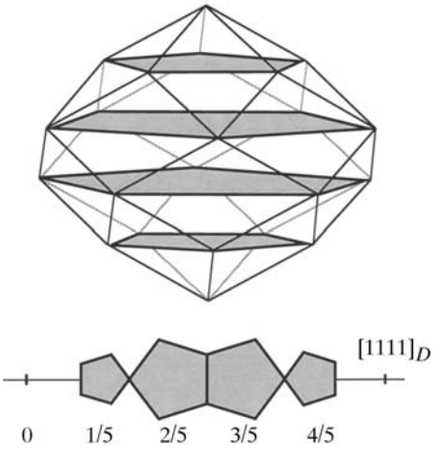

Fig. 4.6.3.15. Atomic surface of the Penrose tiling in the 5D hypercubic description. The projection of the 5D hypercubic unit cell upon $\mathbf{V}^{\perp}$ gives a rhomb-icosahedron (above). The Penrose tiling is generated by four equidistant pentagons (shaded) inscribed in the rhomb-icosahedron. Below is a perpendicular-space projection of the same pentagons, which are located on the $[1111]_D$ diagonal of the 4D hyper-rhombohedral unit cell in the 4D description.

$$W = \begin{pmatrix} a_1^* \cos(2\pi/5) & a_2^* \cos(4\pi/5) & a_3^* \cos(6\pi/5) & a_4^* \cos(8\pi/5) \\ a_1^* \sin(2\pi/5) & a_2^* \sin(4\pi/5) & a_3^* \sin(6\pi/5) & a_4^* \sin(8\pi/5) \\ \hline a_1^* \cos(4\pi/5) & a_2^* \cos(8\pi/5) & a_3^* \cos(2\pi/5) & a_4^* \cos(6\pi/5) \\ a_1^* \sin(4\pi/5) & a_2^* \sin(8\pi/5) & a_3^* \sin(2\pi/5) & a_4^* \sin(6\pi/5) \end{pmatrix}.$$

The 2D Penrose tiling can also be embedded canonically in the 5D space. Canonically means that the 5D lattice is hypercubic and that the projection of one unit cell upon the 3D perpendicular space $\mathbf{V}^{\perp}$, giving a rhomb-icosahedron, defines the atomic surface. However, the parallel-space image $\mathbf{a}_i^*$, $i = 1, \ldots, 4$, with $\mathbf{a}_0^* = -(\mathbf{a}_1^* + \mathbf{a}_2^* + \mathbf{a}_3^* + \mathbf{a}_4^*)$, of the 5D basis $\mathbf{d}_i^*$, $i = 1, \ldots, 4$ is not linearly independent. Consequently, the atomic surface consists of only a subset of the points contained in the rhomb-icosahedron: five equidistant pentagons (one with diameter zero) resulting as sections of the rhomb-icosahedron with five equidistant parallel planes (Fig. 4.6.3.15). The linear dependence of the 5D basis allows the embedding in the 4D space. The resulting hyper-rhombohedral hyperlattice is spanned by the basis $\mathbf{d}_i$, $i = 1, \ldots, 4$, discussed above. The atomic surfaces occupy the positions $p/5(1111)$, $p = 1, \ldots, 4$, on the body diagonal of the 4D unit cell. Neighbouring pentagons are in an *anti* position to each other (Fig. 4.6.3.16). Thus the 4D unit cell is decorated centrosymmetrically. The edge length a_r of a Penrose rhomb is related to the length of physical-space basis vectors a_i^* by $a_r = \tau S$, with the smallest distance $S = (2\tau/5a_i^*)$, $i = 1, \ldots, 4$. The *point density* (number of vertices per unit area) of a Penrose tiling with Penrose rhombs of edge length a_r can be calculated from the ratio of the relative number of unit tiles in the tiling to their area:

$$\rho = \frac{1+\tau}{a_r^2[\sin(\pi/5) + \tau \sin(2\pi/5)]} = (5/2)a_i^{*2}(2-\tau)^2 \tan(2\pi/5).$$

This is equivalent to the calculation from the 4D description,

$$\rho = \frac{\sum_{i=1}^{4} \Omega_{\rm AS}^i}{\Omega_{\rm UC}} = \frac{\sum_{i=1}^{4} (5/2)\lambda^2 \sin(2\pi/5)}{4/[5(5)^{1/2}|a_i^*|^4]} = (5/2)a_i^{*2}(2-\tau)^2 \tan(2\pi/5),$$

where $\Omega_{\rm AS}$ and $\Omega_{\rm UC}$ are the area of the atomic surface and the volume of the 4D unit cell, respectively. The pentagon radii are

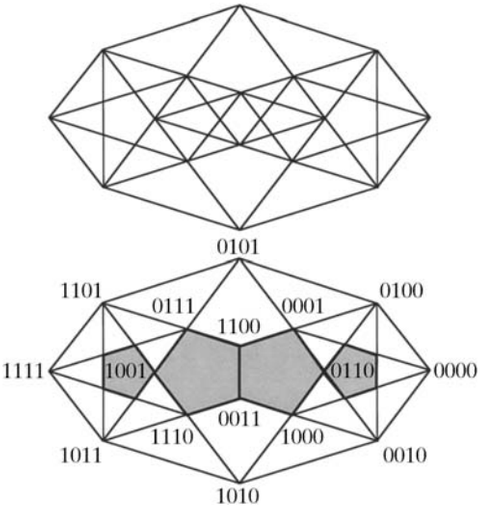

Fig. 4.6.3.16. Projection of the 4D hyper-rhombohedral unit cell of the Penrose tiling in the 4D description upon the perpendicular space. In the upper drawing all edges between the 16 corners are shown. In the lower drawing the corners are indexed and the four pentagonal atomic surfaces of the Penrose tiling are shaded.

$\lambda_{1,4} = 2(2-\tau)/5a^*$ and $\lambda_{2,3} = 2(\tau-1)/5a^*$ for the atomic surfaces in $(p/5)(1111)$ with $p = 1, 4$ and $p = 2, 3$. A detailed discussion of the properties of Penrose tiling is given in the papers of Penrose (1974, 1979), Jaric (1986) and Pavlovitch & Kleman (1987).

4.6.3.3.2.1. Indexing

The indexing of the submodule M_1^* of the diffraction pattern of a decagonal phase is not unique. Since M_1^* corresponds to a $\mathbb{Z}$ module of rank 4 with decagonal point symmetry, it is invariant under scaling by $\tau^n, n \in \mathbb{Z}$: $S^n M^* = \tau^n M^*$. Nevertheless, an optimum basis (low indices are assigned to strong reflections) can be derived: not the metrics, as for regular periodic crystals, but the intensity distribution characterizes the best choice of indexing.

A correct set of reciprocal-basis vectors can be identified experimentally in the following way:

(1) Find directions of systematic absences or pseudo-absences determining the possible orientations of the reciprocal-basis vectors (see Rabson *et al.*, 1991).

(2) Find pairs of strong reflections whose physical-space diffraction vectors are related to each other by the factor τ.

(3) Index these reflections by assigning an appropriate value to a^*. This value should be derived from the shortest interatomic distance S and the edge length of the unit tiles expected in the structure.

(4) The reciprocal basis is correct if all observable Bragg reflections can be indexed with integer numbers.

4.6.3.3.2.2. Diffraction symmetry

The diffraction symmetry of decagonal phases can be described by the Laue groups $10/mmm$ or $10/m$. The set of all vectors $\mathbf{H}$ forms a Fourier module $M^* = \{\mathbf{H}^{\parallel} = \sum_{i=1}^{5} h_i \mathbf{a}_i^* | h_i \in \mathbb{Z}\}$ of rank 5 in physical space which can be decomposed into two submodules $M^* = M_1^* \oplus M_2^*$. $M_1^* = \{h_1\mathbf{a}_1^* + h_2\mathbf{a}_2^* + h_3\mathbf{a}_3^* + h_4\mathbf{a}_4^*\}$ corresponds to a $\mathbb{Z}$ module of rank 4 in a 2D subspace, $M_2^* = \{h_5\mathbf{a}_5^*\}$ corresponds to a $\mathbb{Z}$ module of rank 1 in a 1D subspace. Consequently, the first submodule can be considered as a projection from a 4D reciprocal lattice, $M_1^* = \pi^{\parallel}(\Sigma^*)$, while the second submodule is of the form of a regular 1D reciprocal lattice, $M_2^* = \Lambda^*$. The diffraction pattern of the Penrose tiling decorated with equal point scatterers on its vertices is shown in Fig. 4.6.3.17. All Bragg reflections within

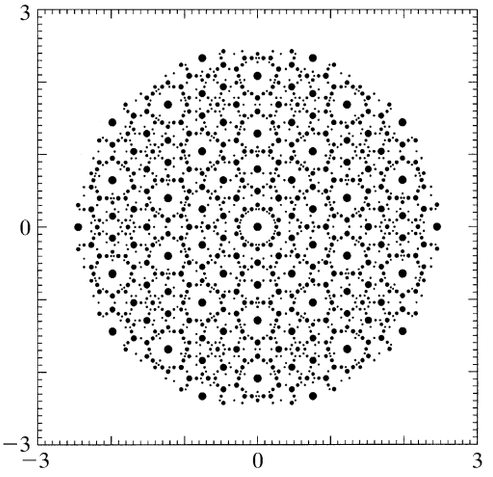

Fig. 4.6.3.17. Schematic diffraction pattern of the Penrose tiling (edge length of the Penrose unit rhombs a_r = 4.04 Å). All reflections are shown within $10^{-2}|F(\mathbf{0})|^2 < |F(\mathbf{H})|^2 < |F(\mathbf{0})|^2$ and $0 \le |\mathbf{H}^{\parallel}| \le 2.5$ Å^{-1}.

$10^{-2}|F(\mathbf{0})|^2 < |F(\mathbf{H})|^2 < |F(\mathbf{0})|^2$ are depicted. Without intensity-truncation limit, the diffraction pattern would be densely filled with discrete Bragg reflections. To illustrate their spatial and intensity distribution, an enlarged section of Fig. 4.6.3.17 is shown in Fig. 4.6.3.18. This picture shows all Bragg reflections within $10^{-4}|F(\mathbf{0})|^2 < |F(\mathbf{H})|^2 < |F(\mathbf{0})|^2$. The projected 4D reciprocal-lattice unit cell is drawn and several reflections are indexed. All reflections are arranged along lines in five symmetry-equivalent orientations. The perpendicular-space diffraction patterns (Figs. 4.6.3.19 and 4.6.3.20) show a characteristic star-like distribution of the Bragg reflections. This is a consequence of the pentagonal shape of the atomic surfaces: the Fourier transform of a pentagon has a star-like distribution of strong Fourier coefficients.

The 5D decagonal space groups that may be of relevance for the description of decagonal phases are listed in Table 4.6.3.1. These space groups are a subset of all 5D decagonal space groups fulfilling the condition that the 5D point groups they are associated with are isomorphous to the 3D point groups describing the diffraction symmetry. Their structures are comparable to 3D hexagonal groups. Hence, only primitive lattices exist. The orientation of the symmetry elements in the 5D space is defined by the isomorphism of the 3D and 5D point groups. However, the action of the tenfold rotation is different in the subspaces $\mathbf{V}^{\parallel}$ and

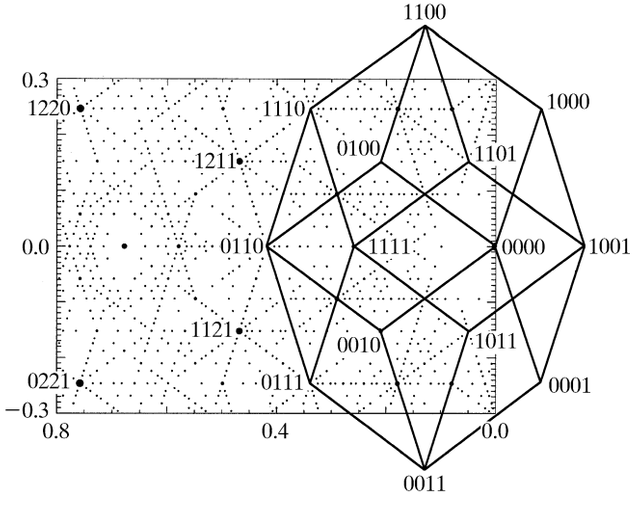

Fig. 4.6.3.18. Enlarged section of Fig. 4.6.3.17. All reflections shown are selected within the given limits from a data set within $10^{-4}|F(\mathbf{0})|^2 < |F(\mathbf{H})|^2 < |F(\mathbf{0})|^2$ and $0 \le |\mathbf{H}^{\parallel}| \le 2.5$ Å^{-1}. The projected 4D reciprocal-lattice unit cell is drawn and several reflections are indexed.

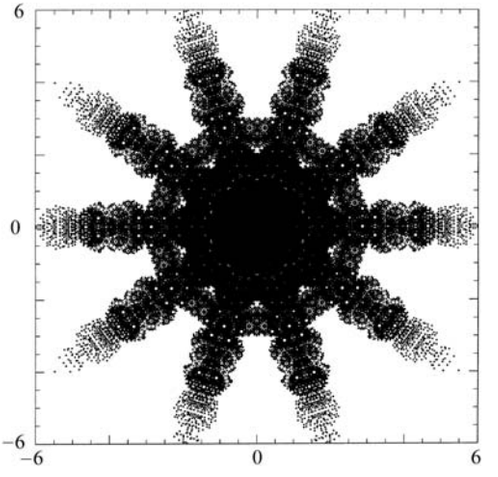

Fig. 4.6.3.19. The perpendicular-space diffraction pattern of the Penrose tiling (edge length of the Penrose unit rhombs a_r = 4.04 Å). All reflections are shown within $10^{-4}|F(\mathbf{0})|^2 < |F(\mathbf{H})|^2 < |F(\mathbf{0})|^2$ and $0 \le |\mathbf{H}^{\parallel}| \le 2.5$ Å^{-1}.

$\mathbf{V}^{\perp}$: a rotation of $\pi/5$ in $\mathbf{V}^{\parallel}$ is correlated with a rotation of $3\pi/5$ in $\mathbf{V}^{\perp}$. The reflection and inversion operations are equivalent in both subspaces.

4.6.3.3.2.3. Structure factor

The structure factor for the decagonal phase corresponds to the Fourier transform of the 5D unit cell,

$$F(\mathbf{H}) = \sum_{k=1}^{N} f_k(\mathbf{H}^{\parallel}) T_k(\mathbf{H}^{\parallel}, \mathbf{H}^{\perp}) g_k(\mathbf{H}^{\perp}) \exp(2\pi i \mathbf{H} \cdot \mathbf{r}_k),$$

with 5D diffraction vectors $\mathbf{H} = \sum_{i=1}^{5} h_i \mathbf{d}_i^*$, N hyperatoms, parallel-space atomic scattering factor $f_k(\mathbf{H}^{\parallel})$, temperature factor $T_k(\mathbf{H}^{\parallel}, \mathbf{H}^{\perp})$ and perpendicular-space geometric form factor $g_k(\mathbf{H}^{\perp})$. $T_k(\mathbf{H}^{\parallel}, \mathbf{0})$ is equivalent to the conventional Debye–Waller factor and $T_k(\mathbf{0}, \mathbf{H}^{\perp})$ describes random fluctuations along the perpendicular-space coordinate. These fluctuations cause characteristic jumps of vertices in physical space (*phason flips*). Even random phason flips map the vertices onto positions which can still be described by physical-space vectors of the type $\mathbf{r} = \sum_{i=1}^{5} n_i \mathbf{a}_i$. Consequently, the set $M = \{\mathbf{r} = \sum_{i=1}^{5} n_i \mathbf{a}_i | n_i \in \mathbb{Z}\}$ of all possible vectors forms a $\mathbb{Z}$ module. The shape of the atomic surfaces corresponds to a selection rule for the positions actually occupied. The geometric form factor $g_k(\mathbf{H}^{\perp})$ is equivalent to the

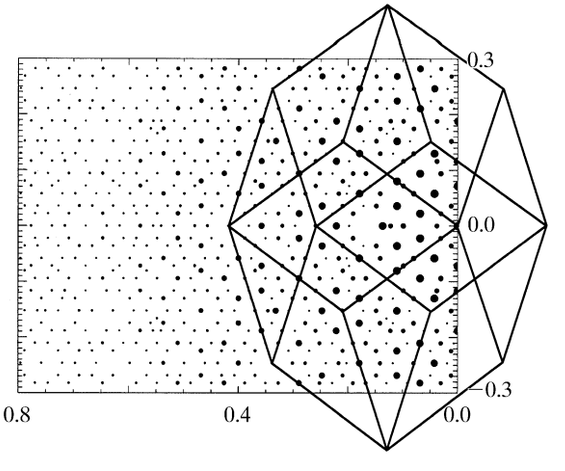

Fig. 4.6.3.20. Enlarged section of Fig. 4.6.3.19 showing the projected 4D reciprocal-lattice unit cell.

Table 4.6.3.1. *3D point groups of order k describing the diffraction symmetry and corresponding 5D decagonal space groups with reflection conditions (see Rabson et al., 1991)*

3D point group	k	5D space group	Reflection condition
$\frac{10}{m}\frac{2}{m}\frac{2}{m}$	40	$P\frac{10}{m}\frac{2}{m}\frac{2}{m}$	No condition
		$P\frac{10}{m}\frac{2}{c}\frac{2}{c}$	$h_1h_2h_2h_1h_5$: $h_5 = 2n$ $h_1h_2\overline{h_2h_1}h_5$: $h_5 = 2n$
		$P\frac{10_5}{m}\frac{2}{m}\frac{2}{c}$	$h_1h_2\overline{h_2h_1}h_5$: $h_5 = 2n$
		$P\frac{10_5}{m}\frac{2}{c}\frac{2}{m}$	$h_1h_2h_2h_1h_5$: $h_5 = 2n$
$\frac{10}{m}$	20	$P\frac{10}{m}$	No condition
		$P\frac{10_5}{m}$	$0000h_5$: $h_5 = 2n$
1022	20	$P1022$	No condition
		$P10_j22$	$0000h_5$: $jh_5 = 10n$
$10mm$	20	$P10mm$	No condition
		$P10cc$	$h_1h_2h_2h_1h_5$: $h_5 = 2n$ $h_1h_2\overline{h_2h_1}h_5$: $h_5 = 2n$
		$P10_5mc$	$h_1h_2\overline{h_2h_1}h_5$: $h_5 = 2n$
		$P10_5cm$	$h_1h_2h_2h_1h_5$: $h_5 = 2n$
$\overline{1}0m2$	20	$P\overline{1}0m2$	No condition
		$P\overline{1}0c2$	$h_1h_2h_2h_1h_5$: $h_5 = 2n$
		$P\overline{1}02m$	No condition
		$P\overline{1}02c$	$h_1h_2\overline{h_2h_1}h_5$: $h_5 = 2n$
$\overline{10}$	10	$P\overline{10}$	No condition
10	10	$P10$	No condition
		$P10_j$	$0000h_5$: $jh_5 = 10n$

Fourier transform of the *atomic surface*, *i.e.* the 2D perpendicular-space component of the 5D *hyperatoms*.

For example, the canonical Penrose tiling $g_k(\mathbf{H}^\perp)$ corresponds to the Fourier transform of pentagonal atomic surfaces:

$$g_k(\mathbf{H}^\perp) = (1/A_{\rm UC}^\perp)\int_{A_k} \exp(2\pi i\mathbf{H}^\perp\cdot\mathbf{r})\ \mathrm{d}\mathbf{r},$$

where $A_{\rm UC}^\perp$ is the area of the 5D unit cell projected upon $\mathbf{V}^\perp$ and A_k is the area of the kth atomic surface. The area $A_{\rm UC}^\perp$ can be calculated using the formula

$$A_{\rm UC}^\perp = (4/25a_i^{*2})[(7+\tau)\sin(2\pi/5) + (2+\tau)\sin(4\pi/5)].$$

Evaluating the integral by decomposing the pentagons into triangles, one obtains

$$g_k(\mathbf{H}^\perp) = \frac{1}{A_{\rm UC}^\perp}\sin\left(\frac{2\pi}{5}\right) \times \sum_{j=0}^{4}\frac{A_j[\exp(iA_{j+1}\lambda_k)-1] - A_{j+1}[\exp(iA_j\lambda_k)-1]}{A_jA_{j+1}(A_j - A_{j+1})}$$

with $j = 0, \ldots, 4$ running over the five triangles, where the radii of the pentagons are λ_j, $A_j = 2\pi\mathbf{H}^\perp\mathbf{e}_j$,

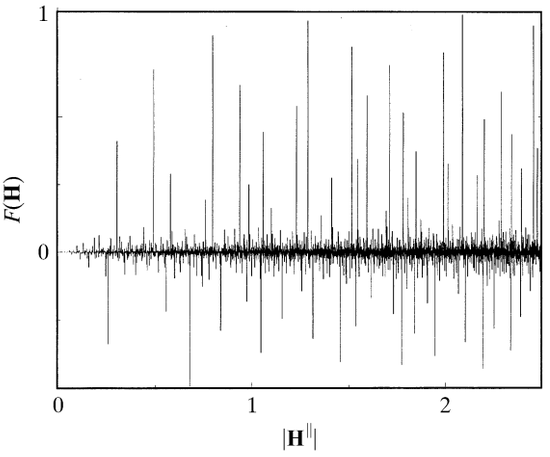

Fig. 4.6.3.21. Radial distribution function of the structure factors $F(\mathbf{H})$ of the Penrose tiling (edge length of the Penrose unit rhombs a_r = 4.04 Å) decorated with point atoms as a function of $\mathbf{H}^\parallel$. All structure factors within $10^{-4}|F(\mathbf{0})|^2 < |F(\mathbf{H})|^2 < |F(\mathbf{0})|^2$ and $0 \le |\mathbf{H}^\parallel| \le 2.5$ Å^{-1} have been used and normalized to $F(0000) = 1$.

$$\mathbf{H}^\perp = \pi^\perp(\mathbf{H}) = \sum_{j=0}^{4} h_j a_j^* \begin{pmatrix} 0 \\ 0 \\ 0 \\ \cos(6\pi j/5) \\ \sin(6\pi j/5) \end{pmatrix}$$

and the vectors

$$\mathbf{e}_j = \frac{1}{a_j^*}\begin{pmatrix} 0 \\ 0 \\ 0 \\ \cos(2\pi j/5) \\ \sin(2\pi j/5) \end{pmatrix} \text{ with } j = 0, \ldots, 4.$$

As shown by Ishihara & Yamamoto (1988), the Penrose tiling can be considered to be a superstructure of a pentagonal tiling with only one type of pentagonal atomic surface in the nD unit cell. Thus, for the Penrose tiling, three special reflection classes can be distinguished: for $|\sum_{i=1}^4 h_i| = m \bmod 5$ and $m = 0$ the class of strong main reflections is obtained, and for $m = \pm1, \pm2$ the classes of weaker first- and second-order satellite reflections are obtained (see Fig. 4.6.3.18).

4.6.3.3.2.4. Intensity statistics

This section deals with the reciprocal-space characteristics of the 2D quasiperiodic component of the 3D structure, namely the Fourier module M_1^*. The radial structure-factor distributions of the Penrose tiling decorated with point scatterers are plotted in Figs. 4.6.3.21 and 4.6.3.22 as a function of parallel and perpendicular space. The distribution of $|F(\mathbf{H})|$ as a function of their frequencies clearly resembles a centric distribution, as can be expected from the centrosymmetric 4D subunit cell. The shape of the distribution function depends on the radius of the limiting sphere in reciprocal space. The number of weak reflections increases to the power of four, that of strong reflections only quadratically (strong reflections always have small $\mathbf{H}^\perp$ components). The radial distribution of the structure-factor amplitudes as a function of perpendicular space clearly shows three branches, corresponding to the reflection classes $\sum_{i=1}^4 h_i = m \bmod 5$ with $|m| = 0$, $|m| = 1$ and $|m| = 2$ (Fig. 4.6.3.23).

The weighted reciprocal space of the Penrose tiling contains an infinite number of Bragg reflections within a limited region of the physical space. Contrary to the diffraction pattern of a periodic

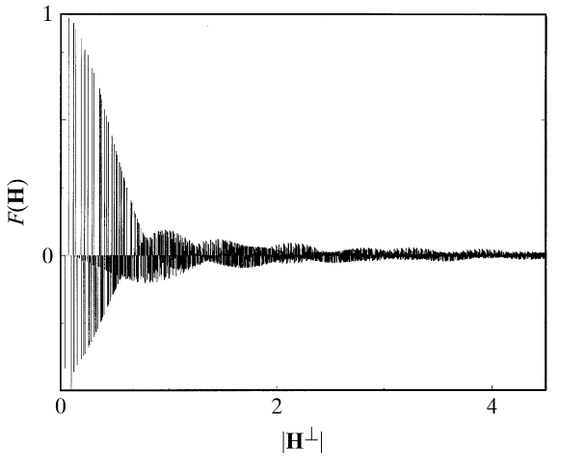

Fig. 4.6.3.22. Radial distribution function of the structure factors $F(\mathbf{H})$ of the Penrose tiling (edge length of the Penrose unit rhombs a_r = 4.04 Å) decorated with point atoms as a function of $\mathbf{H}^{\perp}$. All structure factors within $10^{-4}|F(\mathbf{0})|^2 < |F(\mathbf{H})|^2 < |F(\mathbf{0})|^2$ and $0 \le |\mathbf{H}^{\parallel}| \le 2.5$ Å^{-1} have been used and normalized to $F(0000) = 1$.

structure consisting of point atoms on the lattice nodes, the Bragg reflections show intensities depending on the perpendicular-space components of their diffraction vectors (Figs. 4.6.3.19, 4.6.3.20 and 4.6.3.22).

4.6.3.3.2.5. Relationships between structure factors at symmetry-related points of the Fourier image

Scaling the Penrose tiling by a factor τ^{-n} by employing the matrix S^{-n} scales at the same time its reciprocal space by a factor τ^n:

$$\boldsymbol{S}\mathbf{H} = \begin{pmatrix} 0 & 1 & 0 & \bar{1} & 0 \\ 0 & 1 & 1 & \bar{1} & 0 \\ \bar{1} & 1 & 1 & 0 & 0 \\ \bar{1} & 0 & 1 & 0 & 0 \\ 0 & 0 & 0 & 0 & 1 \end{pmatrix}_D \begin{pmatrix} h_1 \\ h_2 \\ h_3 \\ h_4 \\ h_5 \end{pmatrix} = \begin{pmatrix} h_2 - h_4 \\ h_2 + h_3 - h_4 \\ -h_1 + h_2 + h_3 \\ -h_1 + h_3 \\ h_5 \end{pmatrix}.$$

Since this operation increases the lengths of the diffraction vectors by the factor τ in parallel space and decreases them by the factor $1/\tau$ in perpendicular space, the following distribution of structure-factor magnitudes (for point atoms at rest) is obtained:

$$\begin{aligned} \left|F(S^n\mathbf{H})\right| > \left|F(S^{n-1}\mathbf{H})\right| > \ldots > \left|F(S^1\mathbf{H})\right| > \left|F(\mathbf{H})\right|, \\ \left|F(\tau^n\mathbf{H}^{\parallel})\right| > \left|F(\tau^{n-1}\mathbf{H}^{\parallel})\right| > \ldots > \left|F(\tau\mathbf{H}^{\parallel})\right| > \left|F(\mathbf{H})\right|. \end{aligned}$$

The scaling operations S^n, $n \in \mathbb{Z}$, the rotoscaling operations $(\Gamma(\alpha)S^2)^n$ (Fig. 4.6.3.14) and the tenfold rotation $(\Gamma(\alpha))^n$, where

$$(\Gamma(\alpha)S^2)^n = \begin{pmatrix} 1 & 1 & \bar{1} & \bar{1} & 0 \\ 1 & 2 & 0 & \bar{2} & 0 \\ 0 & 2 & 1 & \bar{1} & 0 \\ \bar{1} & 1 & 1 & 0 & 0 \\ 0 & 0 & 0 & 0 & 1 \end{pmatrix}^n_D,$$

connect all structure factors with diffraction vectors pointing to the nodes of an infinite series of pentagrams. The structure factors with positive signs are predominantly on the vertices of the pentagram while the ones with negative signs are arranged on circles around the vertices (Figs. 4.6.3.24 to 4.6.3.27).

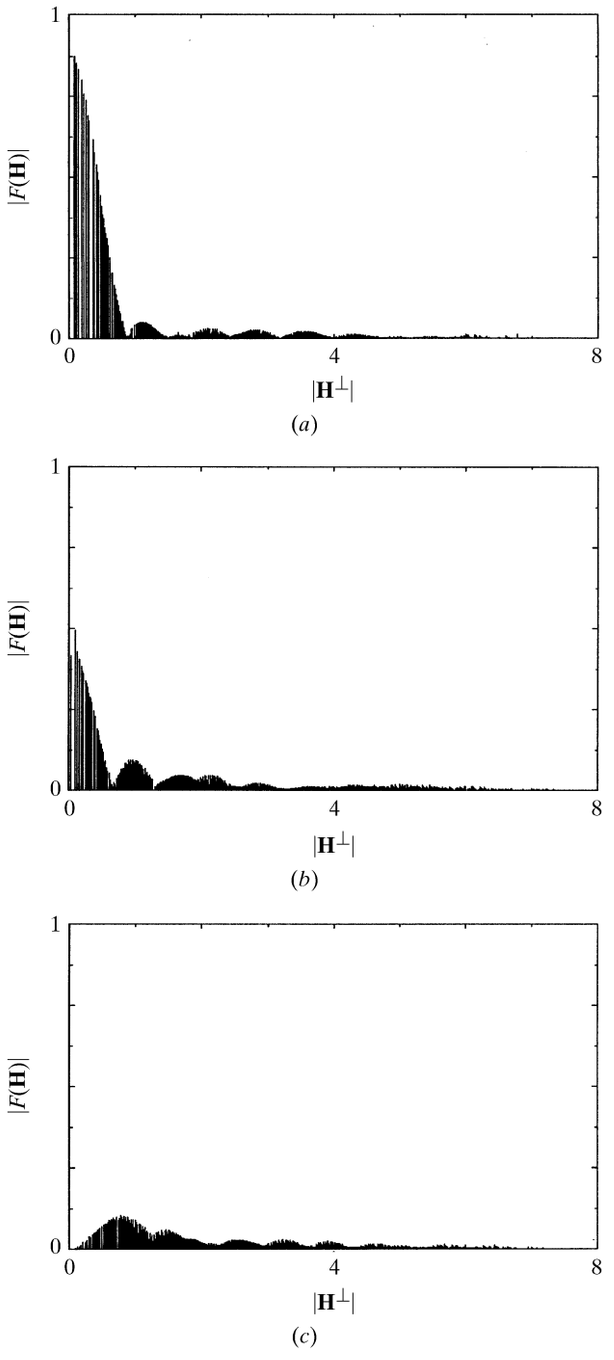

Fig. 4.6.3.23. Radial distribution function of the structure-factor magnitudes $|F(\mathbf{H})|$ of the Penrose tiling (edge length of the Penrose unit rhombs a_r = 4.04 Å) decorated with point atoms as a function of $\mathbf{H}^{\perp}$. All structure factors within $10^{-4}|F(\mathbf{0})|^2 < |F(\mathbf{H})|^2 < |F(\mathbf{0})|^2$ and $0 \le |\mathbf{H}^{\parallel}| \le 2.5$ Å^{-1} have been used and normalized to $F(0000) = 1$. The branches with (*a*) $|\sum_{i=1}^4 h_i| = 0 \bmod 5$, (*b*) $|\sum_{i=1}^4 h_i| = 1 \bmod 5$ and (*c*) $|\sum_{i=1}^4 h_i| = 2 \bmod 5$ are shown.

4.6.3.3.3. Icosahedral phases

A structure that is quasiperiodic in three dimensions and exhibits icosahedral diffraction symmetry is called an icosahedral phase. Its holohedral Laue symmetry group is $K = m\bar{3}\bar{5}$. All reciprocal-space vectors $\mathbf{H} = \sum_{i=1}^6 h_i \mathbf{a}_i^* \in M^*$ can be represented on a basis $\mathbf{a}_1^* = a^*(0, 0, 1)$, $\mathbf{a}_i^* = a^*[\sin\theta\cos(2\pi i/5), \sin\theta\sin(2\pi i/5), \cos\theta]$, $i = 2, \ldots, 6$ where $\sin\theta = 2/(5)^{1/2}$, $\cos\theta = 1/(5)^{1/2}$ and $\theta \simeq 63.44^{\circ}$, the angle between two neighbouring fivefold axes (Fig. 4.6.3.28). This can be rewritten as

references